Available online at www.sciencedirect.com
SCIENCE DIRECT
Journal of the European Ceramic Society 26 (2006) 59–65
www.elsevier.com/locate/jeurceramsoc

Wetting, densification and phase transformation of $La_2O_3/A_2O_3/B_2O_3$-based glass–ceramics

Chih-Lung Chen[a], Wen-Cheng J. Wei[a,*], Andreas Roosen[b]

[a] *Department of Materials Science and Engineering, National Taiwan University, 1 Roosevelt Rd Section 4, Taipei 106, Taiwan, ROC*
[b] *Institute of Materials Science, Glass and Ceramics, University of Erlangen-Nuremberg, Erlangen, Germany*

Received 30 April 2004; received in revised form 10 October 2004; accepted 16 October 2004
Available online 8 December 2004

Abstract

A lead-free, non-alkali La_2O_3–Al_2O_3–B_2O_3 (LAB) glass with Al_2O_3 filler had been investigated for low temperature co-firing ceramic (LTCC) application. The glass forming window and several physical properties of the LAB systems were investigated by ICP, TMA, XRD, DSC, and SEM/EDS. The results show that the densification and crystallization temperatures of LAB/Al_2O_3 were between 700 °C and 950 °C and depended greatly on the formulation. Crystalline phase $LaBO_3$ (LB) and $LaAl_2B_3O_9$ (L2A3B) crystallized starting at 825 °C and 925 °C, respectively. High degree of densification and crystallization of one glass–Al_2O_3 composition (L30A) was observed with the microstructure composed of tabular L2A3B grains interlocking with submicron Al_2O_3 and LB grains.

Keywords: Glass–ceramics; La_2O_3; Al_2O_3; B_2O_3; Wetting; Densification

1. Introduction

Wireless communication has grown rapidly in the past few years. High circuit density packages for miniaturization and for lightweight integrated electronic assembly are required. LTCC technology offers the possibility to produce compact multilayer structures with buried passive components.[1,2] For these reasons, the fabrication of LTCC substrate which relies on the properties of low-melting glassy materials has been much investigated.

Glass–ceramics are polycrystalline materials prepared by the controlled crystallization of highly viscous glass melts,[3] which show wide capability of shape forming. Their properties depend on the glass composition, on the percentage of crystal phases formed, and on the composition of the residual glass and porosity. Therefore, the determination of the degree of crystallization and the investigation of the transformation of the parent glass are very important.[4,5]

Some studies of the atomic structures of lanthanoborate glasses have been reported.[6,7] La_2O_3 has a beneficial effect on the water resistance of alkaline-earth borate optical glasses. Improved durability, high glass-transition temperatures (>600 °C), and expected low electrical conductivities and gas diffusivities make La_2O_3–MO–BO_3 glasses attractive candidate materials for specialized hermetic-sealing applications. On the other hand, Levin et al.[8] reported the system of La_2O_3–B_2O_3 and also showed the phase diagram containing $3La_2O_3{\cdot}B_2O_3$ (3LB), $La_2O_3{\cdot}B_2O_3$ (LB), and $La_2O_3{\cdot}3B_2O_3$ (L3B) compounds. There is liquid phase with a composition near L3B. The boron-rich melt can be formed as low as 1132 ± 5 °C. Very limited information about the glass-forming or crystal regions has been produced. There is no complete ternary phase diagram of La_2O_3–Al_2O_3–B_2O_3 available in the literature.[8,9]

Because of the high melting temperature of the Al_2O_3 grains involved in the LTCC substrate, a sintering process is necessary to transform the LTCC tape to a dense product. The contact angle of the glass on the Al_2O_3 grain surface, which determines the extent of wetting, will depend on both the material characteristics of the glass and the surface properties

* Corresponding author. Fax: +886 2 2363 2684.
E-mail address: wjwei@ccms.ntu.edu.tw (W.-C.J. Wei).

0955-2219/$ – see front matter © 2004 Elsevier Ltd. All rights reserved.
doi:10.1016/j.jeurceramsoc.2004.10.001

of the solid. Furthermore, as the temperature decreases, glass vitrification may be initiated.

The fabrication of glass–ceramic substrates involves powder preparation and shape-forming steps, followed by sintering and crystallization by appropriate heat treatments. The character of sintering and the following crystallization in LAB glass–ceramics thus are interesting and important for the development of a glass–ceramic system. The present work seeks a better understanding on the synthesis of chemically homogeneous LAB glasses and LAB/Al_2O_3 glass–ceramics, including the thermal properties, compositional distribution, wetting measurement, and crystalline behavior. The effect of temperature on the fabrication and crystallization of the LAB system is investigated over a broad temperature interval up to 900 °C.

2. Experimental procedure

2.1. Glass powder

The starting materials included Al_2O_3, La_2O_3, and B_2O_3 powders. The Al_2O_3 powder was high purity APA-0.2 (99.97%, Ceralox Co., Arizona, USA) with a BET surface area of 34.0 m^2/g and an average particle size around 60 nm. La_2O_3 (99.99%, Ya-Guang Co., Chang Sha Corp., China) in sizes less than 325 mesh was used. B_2O_3 powder (99% pure, −40 mesh, ACROS Organics, New Jersey, USA) together with Al_2O_3 and La_2O_3 was dispersed in ethanol. After being mixed for 6 h, the slurries were dried in an oven at 105 °C for 24 h.

The raw powders were weighed according to the compositions shown in Fig. 1 to an accuracy of ±0.2%. The melting temperature of the mixture was set at 1350 °C owing to some Al_2O_3 particles possibly remaining in the LAB glass if the melting was limited to 1300 °C for 1 h. After the 1350 °C treatment, the melts were poured out from the Pt crucible and directly quenched on a Cu plate in air. The glass was ground by ball-milling with alumina grinding media. The glass sample was amorphous by XRD, with no crystalline phase (Al_2O_3 contamination) being observed. The batch composition of melted glasses was measured by ICP, showing B_2O_3 content reduced by 2–3%, and Al_2O_3 increased by <1% with respect to the pre-melt composition. The reduction of B_2O_3 might be a result of sublimation or evaporation during the high-temperature melting (1350 °C).

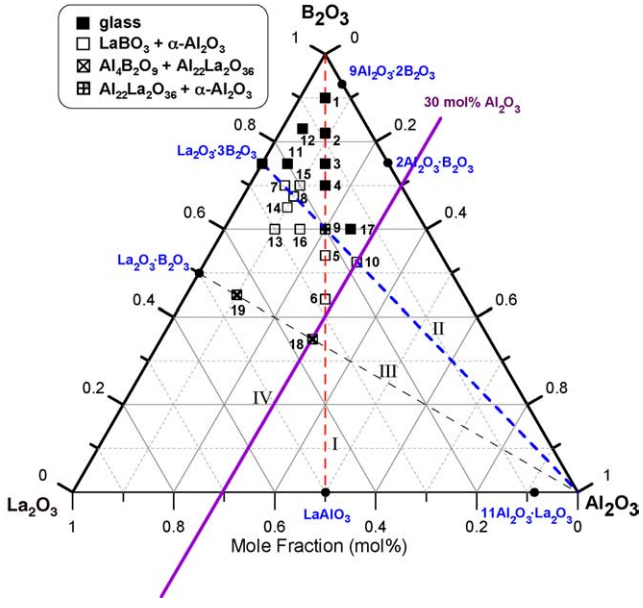

Fig. 1. Ternary compositional diagram of LAB system showing the crystalline conditions of the glasses prepared at 1350 °C/1 h in air.

2.2. Shrinkage measurement

For the measurement of sintering, the sample should have a cross section of not more than 28 mm × 28 mm with a maximum height of 4.5 mm. An optical dilatometer (Nabatherm, model HT 04/17s, Germany) was used with two cameras for the direct observation of the sintering behavior. The same instrument was used to measure the wetting angle. The LAB die-pressed blocks were placed on a flat and polished alumina plate (99.9%, α-Al_2O_3, surface roughness (R_a) 60 nm, average grain size 2.2 μm). The sintering behavior was, in addition, analyzed by using a thermal mechanical analyzer (TMA, SETSYS TMA16/18, SETRAM Co., France), which could operate at temperature up to 1700 °C in atmosphere. The linear expansion or shrinkage of these specimens was recorded. DSC (Netzch DSC404, Germany) was also conducted up to 1050 °C in an air furnace.

2.3. Phase identification and microstructural characterization

The phases of LAB glass or LAB–Al_2O_3 glass–ceramics were identified by an X-ray diffractometer (Philips PW1710, Philips Co., Netherlands). The morphologies of the polished surfaces were analyzed by scanning electron microscopy (Leo Instrument 1530, UK) equipped with an X-ray energy dispersive spectroscopy (EDS, DX-4, EDAX Co., USA).

3. Results and discussion

3.1. Preparation of LAB glass

Fig. 1 shows the compositional diagram of LAB (La_2O_3, Al_2O_3 and B_2O_3) system examined in this investigation. The composition region with filled squares formed transparent glasses when the specimen was quenched in air after melting at 1350 °C for 1 h. On the other hand, the other compositions showed partially crystallization (as determined by X-ray diffraction). In the line I of the ternary diagram, the ratio of La_2O_3 to Al_2O_3 was kept constant (molar ratio 1.0). Lines II and III mean the glass compositions prepared in a propor-

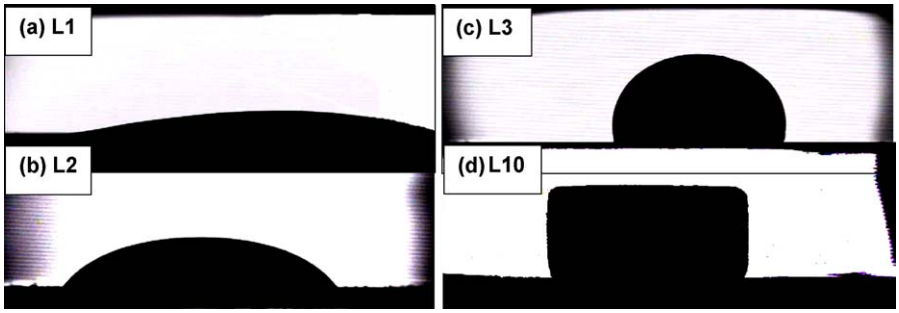

Fig. 2. Optical images of various glasses (a) L1; (b) L2; (c) L3; and (d) L10 on Al_2O_3 wafer, showing the wetting behaviors tested at 850 °C Glass samples, L4 and L5, showed similar images as that of the glass L3.

tion of Al_2O_3 mixed with $La_2O_3{\cdot}3B_2O_3$ and $La_2O_3{\cdot}B_2O_3$, respectively. The B_2O_3 used as a glass former could increase the fluidity of the glass. In order to reduce the sintering temperature and dielectric constant, the Al_2O_3 content in the glass formulation was selected lower than 30 mol% (line IV), as shown in Fig. 1.

Different crystalline phases were founded in the formulations. As the heat treatment was conducted, several crystalline phases (α-Al_2O_3, $LaBO_3$, $Al_{22}La_2O_{36}$) could nucleate from the glassy matrix by the help of the high-melting-temperature ingredients La_2O_3 and Al_2O_3. Two phases, α-Al_2O_3 and $LaBO_3$, were found in the samples L6–L8, L10, and L13–L16. However, L9 showed α-Al_2O_3 and minor $Al_{22}La_2O_{36}$ phase. Basically, the $Al_{22}La_2O_{36}$ phase could be produced in the Al-rich composition according to Al_2O_3–La_2O_3 phase diagram. Several possibilities are responsible for the formation of the $Al_{22}La_2O_{36}$ phase. The phase is the final product of the reaction between Al_2O_3 with La–B–glass by the peritectic reaction:

$$13Al_2O_3 + 2LaBO_3 \rightarrow Al_{22}La_2O_{36} + Al_4B_2O_9 \quad (1)$$

Because $Al_4B_2O_9$ was not identified, the first reaction could be the one occurred at 1350 °C.

3.2. Wetting behaviors of LAB glasses

In order to find out an appropriate composition and sintering temperature for the glass for LTCC, the details of the shrinkage and morphological change of the LAB glasses in the temperatures ranging from 750 °C to 900 °C were recorded by optical dilatometry. A few typical images are shown in Fig. 2. Basically, these glassy specimens could melt on an Al_2O_3 plate and shrink as the temperature reaching 850 °C.

Basically, the L1 and L2 glasses wetted well on the Al_2O_3 plate. The wetting was apparent from 720 °C to 900 °C. It was noted in contrast that the shape of the L10 sample block had no change even at 850 °C. The compositions, e.g., L5, L15 and L10, were accordingly inappropriate in preparing the mixture of glass–ceramics.

The results of optical dilatometric measurement are summarized in Fig. 3. It is essential to have glass wetting at the ceramic filler at the sintering temperature, e.g., ≤900 °C for LTCC application. In Fig. 3(a), the LAB glasses could be

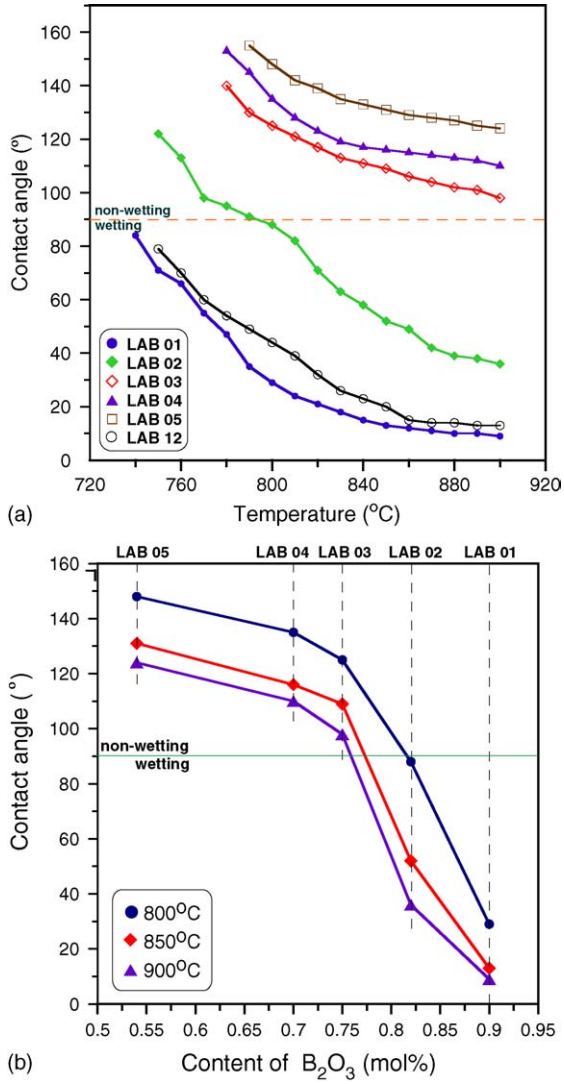

Fig. 3. (a) Contact angle of LAB glasses as a function of the holding temperature in air and (b) wetting behaviors of various glasses (L1, L2, L3, L4 and L5) on Al_2O_3 wafer at 800 °C, 850 °C, or 900 °C in air. The variation of the contact angle measurement is ±3°.

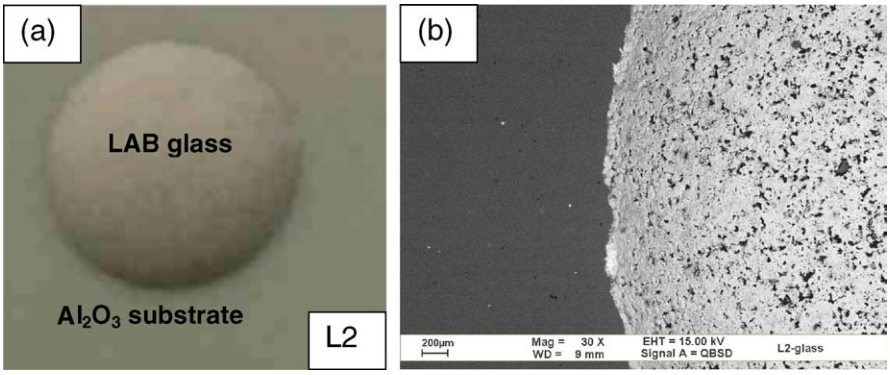

Fig. 4. (a) Optical and (b) SEM pictures illustrating the morphologies of L2 glass on Al_2O_3 wafer after tested at 850 °C.

separated into two categories by the definition of wetting ($\theta < 90°$) and non-wetting ($\theta \geq 90°$). So L1, L12, and some extent of L2 show good wettability at temperatures greater than 800 °C. On the contrary, L3, L4, L5 and L10 appear poor wetting.

A set of typical optical and SEM micrographs of L2 glasses melted on Al_2O_3 at 850 °C are shown in Fig. 4. Those show the nearly dense morphology decorated with tiny pores on the surface (Fig. 4(b)). In contrast, L1 and L12 specimens show different morphology, i.e., cracks, on the top surface. These cracks extend to several hundred micrometers. Such defect would result in many problems, such as poor density and poor dielectric properties. Similar poor features were observed near the interface between the L1 and L12 glasses and the Al_2O_3 substrate.

In general, the B_2O_3 modifier could increase the fluidity of the glass and the pores were correspondingly coalesced during melting. In addition, increase of the B_2O_3 content can lower the dielectric constant of the sample. However, the vaporization of B_2O_3 and the possible cracking induced by glass reaction may degrade the sintering properties. Apparently, the contact angles of LAB glasses show temperature- and B_2O_3-dependence. On the other hand, Al_2O_3 is used as a filler to improve the mechanical strength of the glass. It is necessary to find a compromise for the contents of B_2O_3 and Al_2O_3 in the fabrication of LTCC materials. Therefore, the L2 glass (La_2O_3:10%, Al_2O_3:10%, B_2O_3:80%) is preferred in this study.

3.3. Thermal behavior

Thermal analysis of various LAB glass is shown in Figs. 5–7. Fig. 5 shows the DSC result of amorphous L2 glass at a heating rate of 10 °C/min tested in air. Distinct glass-transition (first endothermic peak) and exothermic crystallization of L2 sample are observed from the curve. The endothermic reaction at 697 °C in the DSC curve corresponds to the glass-transition temperature (T_g). The first exothermic peak depicts the onset temperature of crystallization (T_o) at 822 °C. The crystallization peak temperature is at 840 °C (T_p).

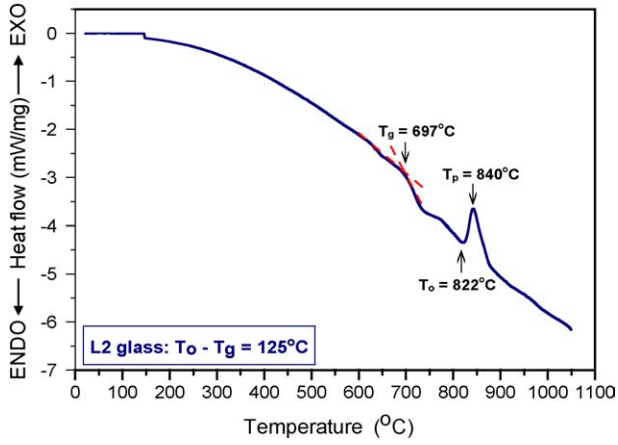

Fig. 5. DSC curve of L2 glass powder tested at a heating rate of 10 °C/min; depicting T_g: transition temperature (or onset of viscous-flow); T_o: onset temperature and T_p: peak temperature in the diagram.

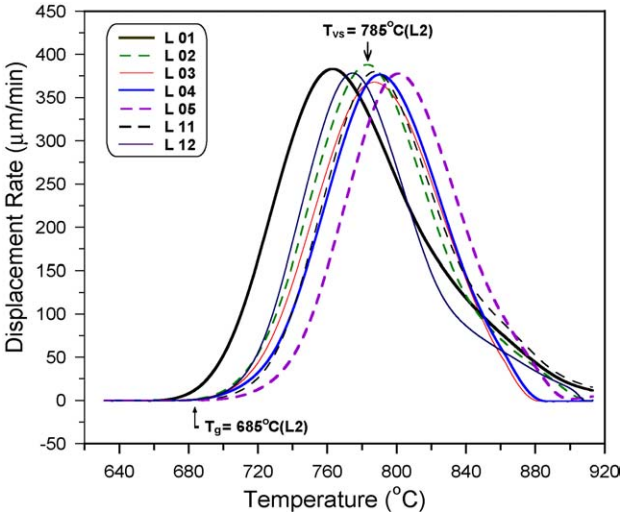

Fig. 6. Differential TMA curves showing the shrinkage rate of LAB glasses as a function of temperature with a load of 10 gf (1.2 kPa) and a heating rate of 10 °C/min to 900 °C in air. T_{vs} is the temperature of maximum shrinkage rate.

The shrinkage results of seven glasses are shown in Fig. 6. The DTMA curves represent the derivative of the displacement with respect to sintering time under a continuous heating rate of 10 °C/min. The threshold temperature 685 °C of the L2 curve (nearly equal to T_g in Fig. 5) is marked on the TMA curve in Fig. 6. The onset of viscous-flow is consistent with the T_g (697 °C). The maximum shrinkage rate temperature, T_{vs} (785 °C) is also marked on the DTMA curve. There is a processing region from 785 °C to 822 °C, which can be utilized for liquid phase (viscous) sintering.

3.4. Effects of Al_2O_3 filler

In order to understand the interaction and effect of Al_2O_3 filler to the glass matrix, two fundamental tests were conducted. First, a linear shrinkage of the glass–ceramic as a function of heating temperature for the L30A (glass with 30% Al_2O_3), L40A and L50A was measured, as shown in Fig. 7. The L40A and L50A show two-step shrinkage, and display different linear shrinkages of 14.1% and 9.9%, respectively. We thought that the shrinkage of L40A and L50A in the early stages of sintering at temperatures between the T_g (glass-transition temperature) and T_{vs} (maximum shrinkage rate temperature) should bring about insignificant shrinkage. Initially, the sintering might reduce the capillary driving force for densification first by increasing the necking between the glass particles. As the amount of Al_2O_3 filler is ≥40%, the melting glass could not wet the Al_2O_3 particles completely, and the Al_2O_3 particles therefore move and rearrange slowly. Fast shrinkage of L40 and L50 is hence delayed. The L30A shows in contrast only one-step shrinkage and the final shrinkage is 19.3%.

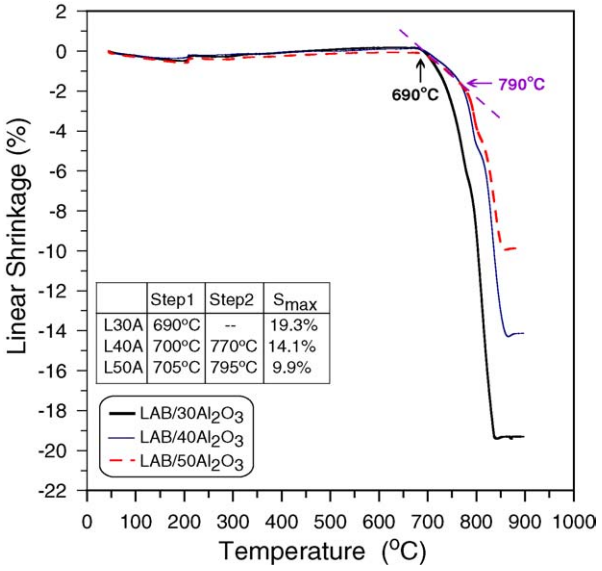

Fig. 7. TMA dilatometric curves of three glass–ceramic samples showing the linear shrinkage of the specimens plotted against sintering temperature.

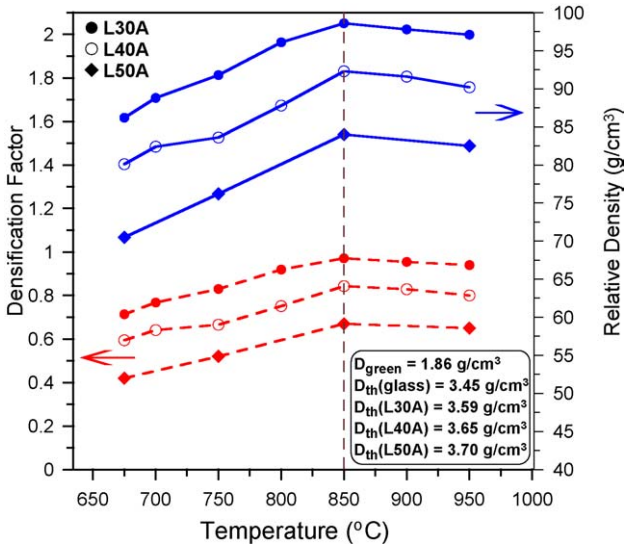

Fig. 8. Density and densification factor (DF) of L30A, L40A and L50A as a function of sintering temperature. The sintering was conducted all for 30 min.

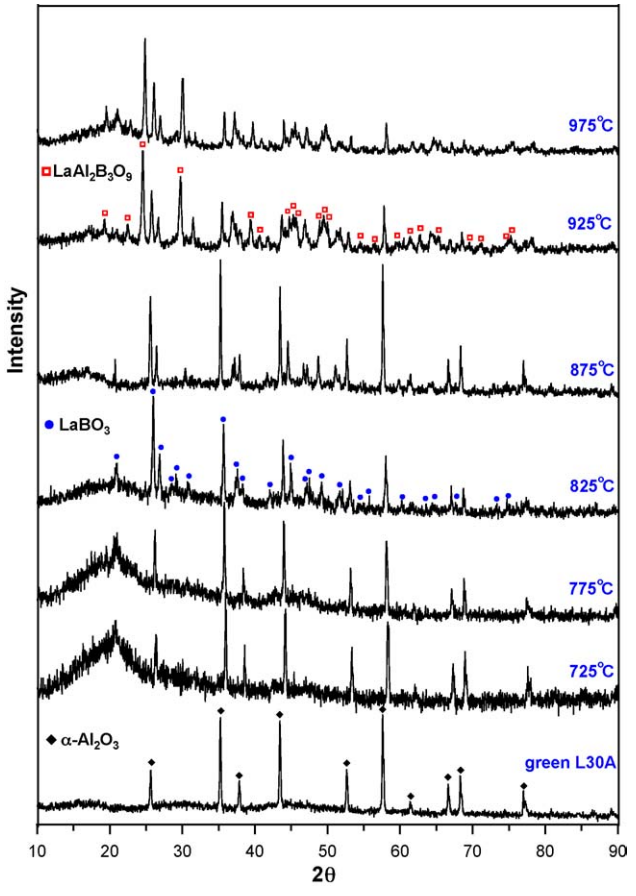

Fig. 9. XRD spectra of the L30A glass–ceramics heat-treated at different temperatures for 30 min in air.

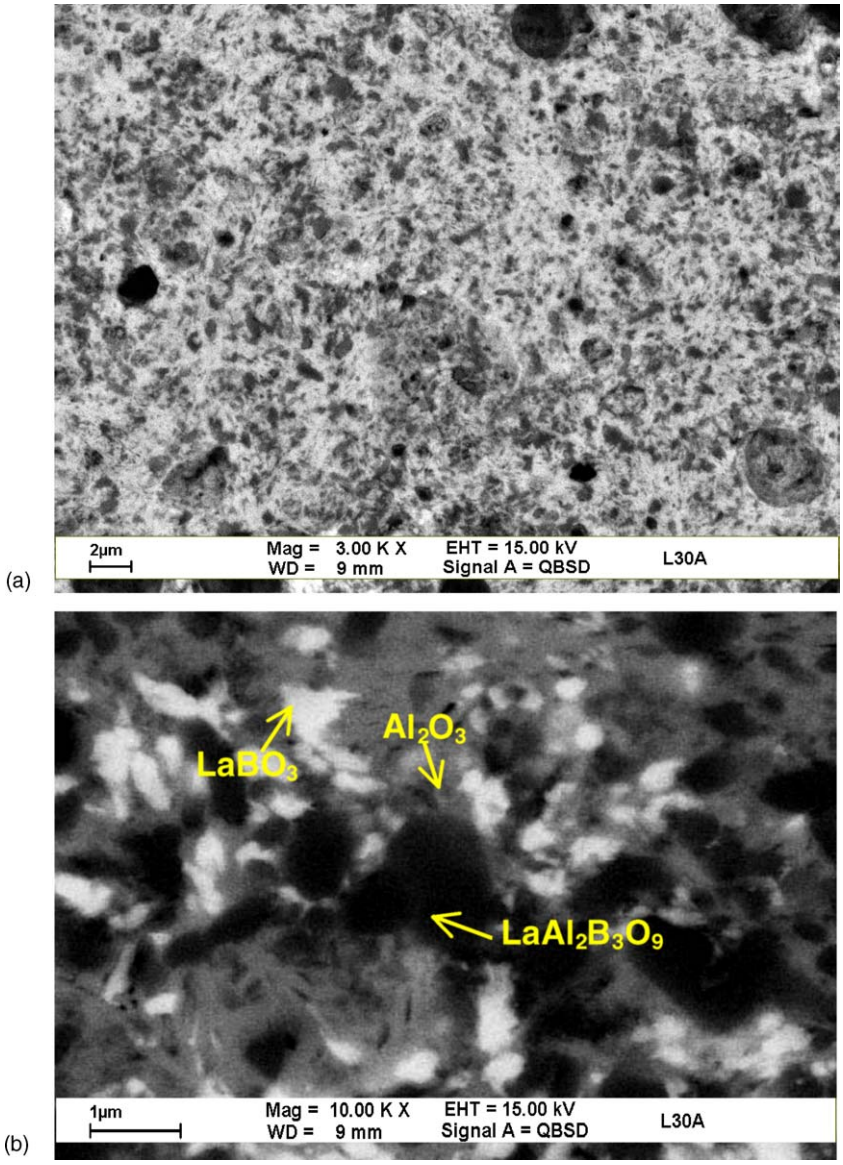

Fig. 10. SEM micrographs imaging by BSE mode showing the microstructure of the L30A sintered at 850 °C for 30 min in air. The description of pores, Al_2O_3 filler, $LaBO_3$ and $LaAl_2B_3O_9$ is shown in the text.

The dilatometric curves suggested that the sudden stop in the final stage of shrinkage (above 820 °C) corresponded to the crystallization of a new phase. The temperature 690 °C led to rapid particle rearrangement during liquid phase sintering of the L2–glass–ceramic. On the other hand, the L40A and L50A commenced apparent sintering at around 790 °C. As a consequence, the sintering of L40A and L50A was stopped and their densification was not completed. The L30A composition showed the lowest initial sintering temperature and extended shrinkage in this study.

Fig. 8 shows the densification results of different compositions (L30A, L40A and L50A) sintered either at 675 °C or at the temperatures up to 950 °C for 30 min. A nearly full density (98.6% D_{th}) of L30A can be obtained at 850 °C. In order to compare the densification behavior among different specimens, a densification factor (DF) was introduced.[10]

$$\mathrm{DF} = \frac{D_b - D_g}{D_{th} - D_g} \tag{2}$$

where D_b is the bulk density of the sintered sample, D_g is the green density and D_{th} is the theoretical density of the composite calculated by the mixing rule. The DF is shown in Fig. 8 for the samples sintered at temperatures from 675 °C to 950 °C. The densification factor of L30A was 0.97. The DF increased rapidly initially and then leveled to a value close to 1.0.

The densification pattern of L30A and L40A is different from that of L50A. The densification of L30A is owing to viscous-flow, resulting in coalescence of filler particles and

the remove of pores in the compact bodies. Therefore, the ratio between glass/filler and the wetting/viscosity of the glass has a great influence on the densification behavior. Therefore, L30A appears the optimal composition that promises a good densification at 850 °C in 30 min.

3.5. Phase and microstructural evolution of L30A sample

In order to verify the dependence of crystallization on temperature, a series of XRD tests for L30A glass–ceramics was conducted, as represented in Fig. 9. Except for the α-Al_2O_3 phase, no crystalline peaks were identified in the green L30A sample. As the temperature increased, an additional crystalline phase, $LaBO_3$, found at temperatures from 825 °C to 925 °C (i.e., above T_o). Moreover, a $LaAl_2B_3O_9$ phase started to form above 925 °C, but the $LaBO_3$ peaks became weaker. The formation of $LaAl_2B_3O_9$ (L2A3B) might involve the reaction of Al_2O_3 grains with La–B–O glass or with the $LaBO_3$ phase. The dissolution of Al_2O_3 in the glass matrix or the reaction with $LaBO_3$ at higher firing temperature is possible.

Two magnified back-scattered electron (BSE) images of a polished surface of the L30A sample are shown in Fig. 10. The particle size and morphologies of the Al_2O_3 grain appear as the darkest contrast, as proven by EDS analysis. Besides, nearly spherical (the brightest features) and tabular (grey contrast) grains could be clearly distinguished. Most of the isolated (nearly equiaxial) Al_2O_3 particles were well dispersed in the matrix. The temperature 850 °C was appropriate for densification, and kept the Al_2O_3 particles least reacted with the glass. The distributions of the flaky crystals, Al_2O_3, and $LaBO_3$ grains were homogeneous, and showed interlocking microstructure. Very little glass was left in the matrix.

4. Conclusions

The $La_2O_3/Al_2O_3/B_2O_3$-based glass–ceramic system has been fabricated and investigated. Appropriate glass melting temperature and formulation were determined and selected. Dense glass–ceramic bulky samples could be prepared to a density better than 98%. The results can be summarized as follows:

1. The processing window of the LAB glasses with compositions of Al_2O_3 less than 30 mol%, La_2O_3 less than 25 mol%, and B_2O_3 more than 70% were used. Some crystalline phases, including α-Al_2O_3, $LaBO_3$, $Al_4B_2O_9$, and $Al_{22}La_2O_{32}$ were identified in the LAB formulation at 1350 °C.
2. The initial shrinkage temperature of the LAB glasses could be as low as 690 °C, and was dependent on the content of B_2O_3.
3. The wetting behavior of the LAB glasses up to 900 °C has been investigated. The L2 (La_2O_3: 10%, Al_2O_3: 10%, B_2O_3: 80%) glass showed an optimal wetting behavior in the ternary LAB system.
4. The L2 glass mixed with 30 mass% of Al_2O_3 filler (L30A) was the best composition for 850 °C sintering. The sintering behavior could reach 98.6% D_{th} and 19.3% linear shrinkage at 850 °C for 30 min.
5. Two crystalline phases, $LaBO_3$ and $LaAl_2B_3O_9$, were crystallized in the L30A glass–ceramic during sintering at ≥825 °C and ≥925 °C, respectively.
6. The microstructure of L30A sintered at 850 °C showed that tabular $LaAl_2B_3O_4$, equiaxial Al_2O_3 and $LaBO_3$ grains formed an interlocking microstructure. Very little glass was found in the sintered glass–ceramic sample.

Acknowledgment

The authors like to thank Institute of Glass and Ceramics at University of Erlangen-Nuremberg, Germany, for kindly providing laboratory facility and the financial support from DAAD (PPP091004476) in Germany and NSC (92-2911-I-002-011) in Taiwan.

References

1. Rubioa, M. R. G., Vallejosb, P. E., Lagunac, L. S. and Avile, J. J. S., Overview of low temperature co-fired ceramics tape technology for meso-system technology (MsST). *Sens. Actuators*, 2001, **A89**, 222–241.
2. Dernovsek, O., Naeini, A., Preu, G., Wersing, W., Eberstein, M. and Schiller, W. A., LTCC glass–ceramic composites for microwave application. *J. Eur. Ceram. Soc.*, 2001, **21**, 1693–1697.
3. Edress, H. J., Smith, A. C. and Hendry, A., A rule-of-mixtures model for sintering of particle-reinforced ceramic–matrix composites. *J. Eur. Ceram. Soc.*, 1998, **18**, 275–278.
4. Eberstein, M., Schiller, W., Dernovsek, O. and Wersing, W., Adjustment of dielectric properties of glass ceramic composites via crystallization. *Glass Sci. Technol.*, 2000, **C1**, 73.
5. Tummala, R. R., Ceramic and glass–ceramic packaging in the 1990s. *J. Am. Ceram. Soc.*, 1991, **74**, 895–908.
6. Chakraborty, I. N. and Day, D. E., Effect of R^{3+} ions on the structure and properties of lanthanum borate glasses. *J. Am. Ceram. Soc.*, 1985, **68**(12), 641–645.
7. Brow, R. K., Tallant, D. R. and Turner, G. L., Raman and ^{11}B nuclear magnetic resonance spectroscopic studies of alkaline-earth lanthanoborate glasses. *J. Am. Ceram. Soc.*, 1996, **79**(9), 2410–2416.
8. Levin, E. M., Robbins, C. R. and Waring, J. L., Immiscibility and the system lanthanum oxide-boric oxide. *J. Am. Ceram. Soc.*, 1961, **44**(2), 89.
9. Brow, R. K., Tallant, D. R. and Turner, G. L., Polyhedral arrangements in lanthanum aluminoborate glasses. *J. Am. Ceram. Soc.*, 1997, **80**(5), 1239–1244.
10. Yan, S. M. and Jose, M. F., The densification and morphology of cordierite-based glass–ceramics. *Mater. Lett.*, 2001, **47**, 833–836.